DOI 10.1007/s11141-022-10185-0
Radiophysics and Quantum Electronics, Vol. 64, No. 12, May, 2022
(Russian Original Vol. 64, No. 12, December, 2021)

QUASI-OPTICAL SUB-DOPPLER LAMB-DIP SPECTROMETER

R. A. Alekseev,[1] I. V. Lapkin,[1] A. V. Lapinov,[1,2] *
T. A. Khabarova,[1] G. Yu. Golubyatnikov,[1]
A. F. Andriyanov,[1] A. P. Schkaev,[1] and
P. M. Zemlyanukha [1]

UDC 535.31+535.34

We describe a new sub-Doppler spectrometer with an enlarged gas cell, which was created at the IAP RAS for high-precision laboratory measurements of molecular transitions at millimeter and submillimeter wavelengths in the interests of radio astronomy. By using a larger diameter with a shortened cell length, a calibrated attenuator for radiation power adjustment, and synthesizers with lower phase noise, it was possible to eliminate a number of shortcomings of the previous spectrometer and not only to measure with high accuracy the transition frequencies of a number of molecules taking into account hyperfine splitting, but also to study their shifts due to both pressure and radiation power. In particular, information about precise frequencies will be used to examine the inner dynamics in the star-forming regions, and also to search for variations of fundamental constants. The principle of frequency-independent cell-aperture irradiation was employed when the optical scheme of the spectrometer was designed. The examples show Lamb-dip measurements of the hyperfine structure in the CH_3CN and HNCO molecular lines.

1. INTRODUCTION

Currently, due to a significant increase in the sensitivity of radio-astronomy receivers, the accuracy of measuring the centers of molecular lines in the interstellar medium, especially in dense cold cores of dark clouds at the prestellar stage, in the Doppler velocity scale is less than or of the order of 1 m/s, i. e., the relative accuracy does not exceed $3 \cdot 10^{-9}$. This inevitably imposes heavy demands on laboratory spectroscopy, which should provide measurements of transition frequencies not with lower, but preferably much higher accuracy (see, in particular, examples of using high-precision laboratory frequency measurements to analyze inner motion in dark clouds [1, 2] and refine laboratory frequencies of other molecules based on radio astronomy measurements [3]). Unfortunately, with conventional Doppler spectroscopy, typical laboratory errors in measuring the centers of lines in the range from centimeter to submillimeter wavelengths vary from tens to hundreds of kilohertz, and frequently a few megahertz [4].

Today there are several ways to increase the accuracy of measurements, one of which is the method of nonlinear sub-Doppler Lamb-dip spectroscopy. Fundamentals of this method in relation to optics are most fully described in [5]. The essence of this method is the formation of narrow dips on a wide Doppler circuit with double-pass propagation of radiation, when, as a result of selection of the power of the probed radiation and gas pressure in the cell responsible for radiation absorption and collisional relaxation, respectively, it is

* lapinov@ipfran.ru

[1] Institute of Applied Physics of the Russian Academy of Sciences; [2] Minin University, Nizhny Novgorod, Russia. Translated from Izvestiya Vysshikh Uchebnykh Zavedenii, Radiofizika, Vol. 64, No. 12, pp. 971–982, December 2021. Russian DOI: 10.52452/00213462_2021_64_12_971 Original article submitted February 8, 2022; accepted February 28, 2022.

possible to saturate the lines near the zero Doppler velocity of molecules and measure the transition frequencies, by using modulation, orders of magnitude more accurately in comparison with Doppler spectroscopy. Since when radiation passes along the cell in opposite directions, two independent groups of molecules that are in resonance with the radiation and Doppler shifted in opposite directions always exist at any frequency detuning from the line center, and they are the same group of molecules at the center transition frequency, then exactly this forms a dip in absorption under saturation conditions only near the line center. The width of the resulting dips is directly proportional to the gas pressure in the cell, the broadening of the lines by radiation, and the frequency of collisions of molecules with walls, and inversely proportional to the time of passage of molecules across the beam, and the line shape is strongly influenced by all possible nonlinear effects due to the interaction of harmonics during modulation, the impact of standing waves, the parameters of frequency modulation, and phase noise of a narrow-band probing oscillator. Therefore, this method is quite laborious and relatively little popular despite the enormous profit in accuracy. In addition to our team, which has been performing such measurements at the IAP RAS for a number of years in the millimeter and submillimeter wavelength ranges [6–9], numerous studies in this field are carried out by G. Cazzoli and C. Puzzarini at the University of Bologna (Italy), starting with their paper [10], in which the features of measurements at the second harmonic of the modulation frequency are described in detail. The full list of their works on this subject includes dozens of publications. Similar measurements were also performed with the participation of IAP RAS staff at the University of Cologne (see, e. g., [11] and other publications), the Kiel University [12] in Germany, and others. In addition, it is worth noting similar studies of the Ukrainian group, which were carried out until recently both in Kharkiv and at the Lille 1 University (France) [8, 9, 13, 14].

This paper describes a developed and manufactured Doppler spectrometer based on the effect of nonlinear saturation of spectral transitions by the Lamb-dip method using a gas cell with a diameter of 400 mm. The need for such a development is due to previous experience. Earlier, a wide-band resonator-free Doppler spectrometer of millimeter and submillimeter wavelength ranges with a gas cell 113 mm in diameter and 2000 mm long was created at the IAP RAS [6]. However, the measurements of transitions in HC_3N and OCS molecules based on this spectrometer [7] showed distortion of the line shape for a number of frequencies due to the large optical depth, and in some cases, significant nonlinear distortions due to radiation saturation. An impact on the line width of the molecule collisions with walls and a short transit time across the beam due to the insufficient cell diameter also took place. A new spectrometer with a gas cell of enlarged diameter was developed to reduce these effects. A vacuum chamber, originally made for a cooled radio astronomy receiver, was used as a cell.

Formally, the coefficient of reducing the specific radiation power with a new cell can reach a value determined by the ratio between cross-sectional areas of these cells. The actual value of the signal power, in addition to the cell sizes, depends on the effective radius of the propagating beam and is determined by the irradiating optics. The standard approach with minimizing signal losses over the entire optical path length requires the selection of the aperture of all elements, including the cell itself, from the condition $D \geq 5w$, where D is the geometric diameter of the aperture and w is the radius of the Gaussian beam for the amplitudes of electric and magnetic fields at the 1/e level. This approximation is used, in particular, to calculate quasi-optical paths in the ALMA [15] and APEX [16, 17] observatories. However, for our facility, this condition, applicable outside the gas cell, somewhat contradicts the most efficient use of its volume. Therefore, one of the goals of this project was to implement the frequency independence of the path in the operating range 75–115 GHz with a slightly increased Gaussian beam. Herein, in order to avoid undesirable reflections from the metal flange of the cell and related standing waves, the optical design version was chosen in the approximation of the fundamental Gaussian mode when irradiating the edge of the cell at a level of -9 dB in power, which corresponds to the cell diameter $4w$. As for the aperture of the mirrors of the quasi-optical path, their sizes were calculated from the condition $D \geq 5w$ that is equivalent to irradiation at a level no higher than -13.6 dB.

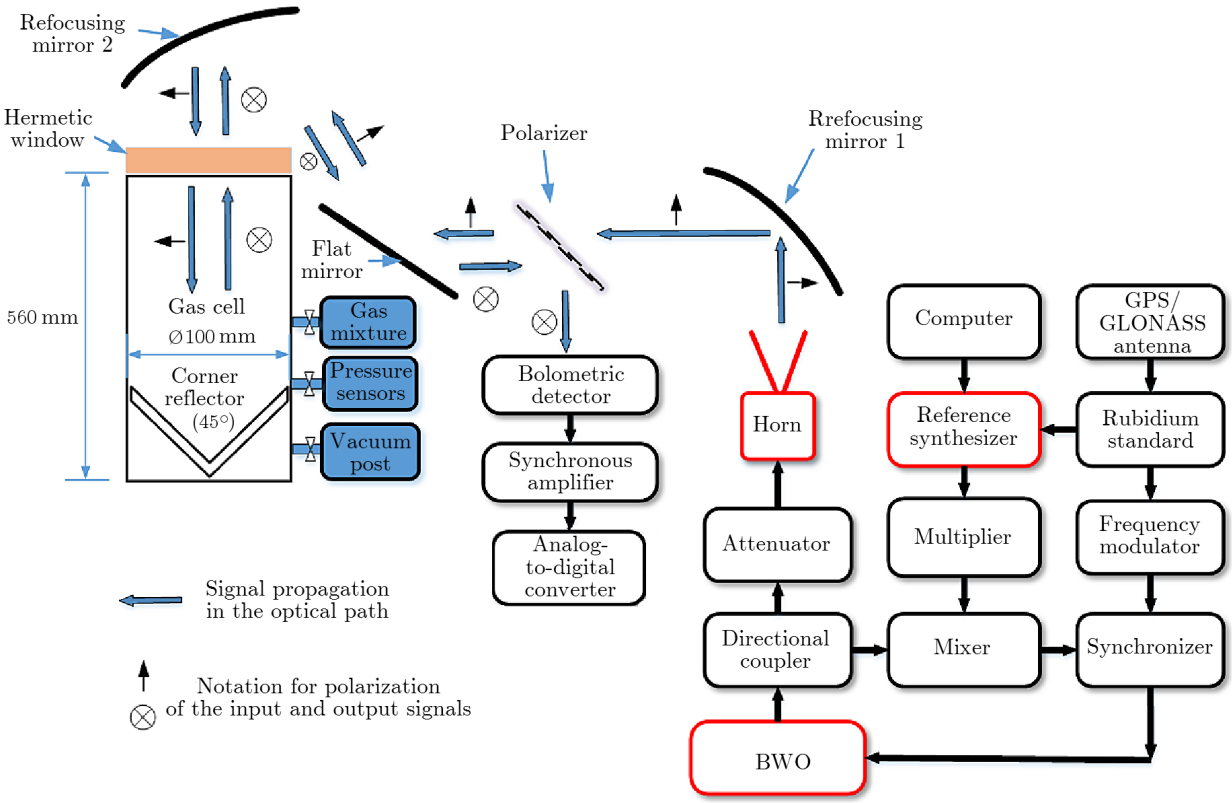

Fig. 1. Block diagram of a sub-Doppler spectrometer.

2. OPTICAL DESIGN OF THE SPECTROMETER

Figure 1 shows a block diagram of a spectrometer with information control and acquisition systems, phase stabilization of a backward wave oscillator (BWO), and a quasi-optical system shown in Fig. 2. The principle of operation of such a spectrometer was described earlier in [6]. Therefore, in what follows we will speak about a quasi-optical system.

The system elements and the optical path were designed in the Gaussian optics approximation [18]. We assume that the base plane is the aperture of a horn with a Gaussian beam specified by the parameter q using the expression [19, 20]

$$\frac{1}{q} = \frac{1}{R} - i\frac{\lambda}{\pi w^2}, \tag{1}$$

where R is the radius of the phase front curvature, w is the radius of the Gaussian beam approximating the field distribution at the 1/e level, and λ is the wavelength.

To trace radiation, it is convenient to use the method of ray $ABCD$-matrices [16, 17, 20] corresponding to propagation in free space, as well as reflection from elliptical mirrors. Figure 3 shows schematically the Gaussian beam path. Since the beam is reflected from the second refocusing mirror twice, two optical elements will correspond to this element in the equivalent scheme at a distance equal to the double passage of the path from the mirror to the corner reflector at the bottom of the cell. Thus, this scheme consists of four ellipsoidal reflectors, which are described using the ray matrices $\mathbf{M}_2$, $\mathbf{M}_4 = \mathbf{M}_6$, and $\mathbf{M}_8$. The transformation of the parameter q can be calculated using the $ABCD$ law [20]:

$$q_2 = \frac{Aq_1 + B}{Cq_1 + D}. \tag{2}$$

We now consider the path from the horn to the second focusing mirror (see Fig. 3). In this case, the ray

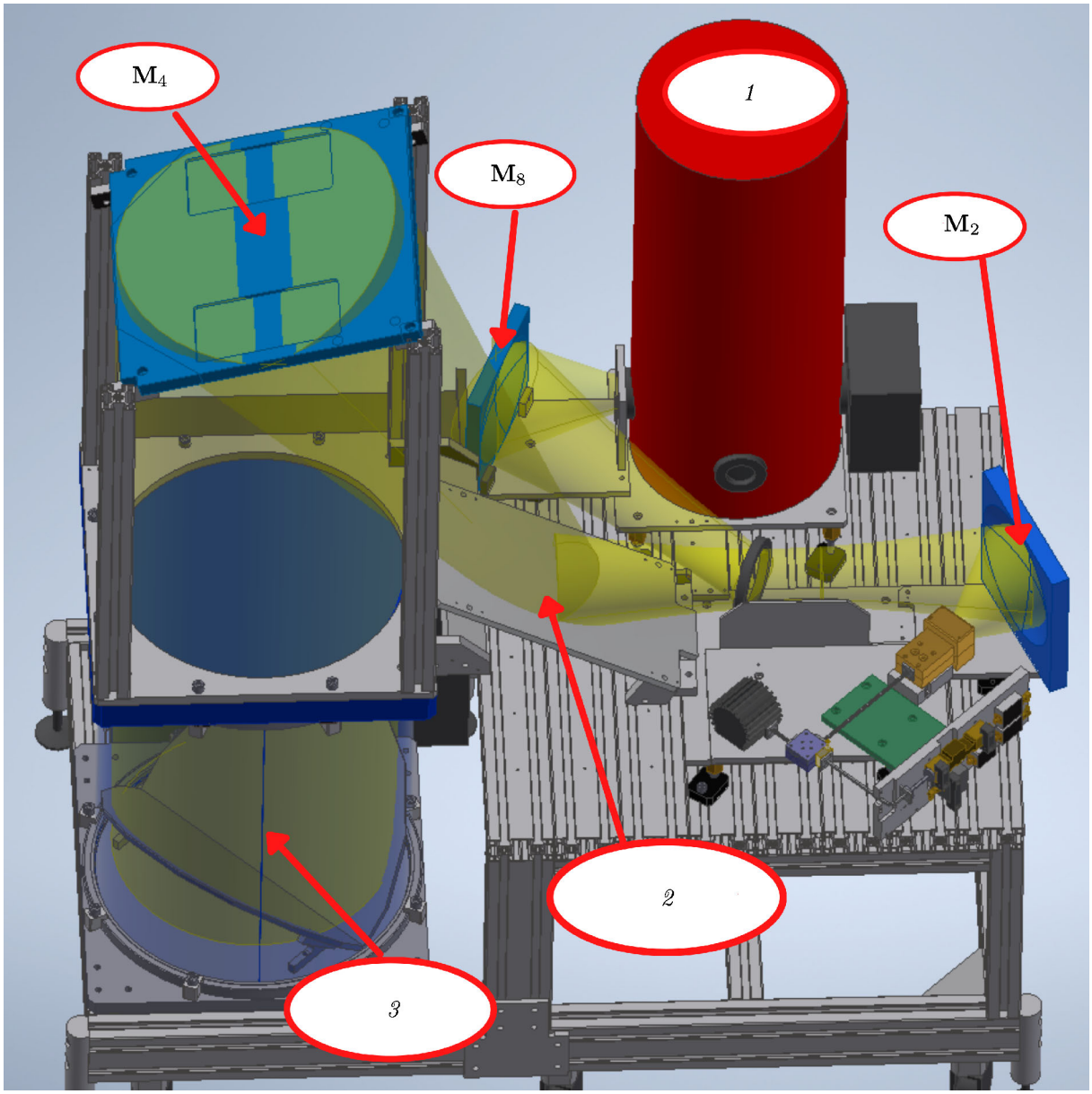

Fig. 2. Quasi-optical path in a millimeter spectrometer: bolometer (*1*), flat mirror (*2*), and corner reflector (*3*). The $\mathbf{M}_2$, $\mathbf{M}_4$, and $\mathbf{M}_8$ matrices in the text correspond to the ellipsoidal reflector indicated in the figure.

matrix $ABCD$ is represented as

$$\mathbf{M} = \begin{pmatrix} 1 & d_2 \\ 0 & 1 \end{pmatrix} \begin{pmatrix} 1 & 0 \\ -\frac{1}{f_1} & 1 \end{pmatrix} \begin{pmatrix} 1 & d_1 \\ 0 & 1 \end{pmatrix} = \begin{pmatrix} 1 - \dfrac{d_2}{f_1} & d_2 + d_1\left(1 - \dfrac{d_2}{f_1}\right) \\ -\dfrac{1}{f_1} & 1 - \dfrac{d_1}{f_1} \end{pmatrix}. \tag{3}$$

Nullifying the element B in the matrix to fulfill the condition of frequency independence [21], we obtain the equation for d_2:

$$d_2 = -\frac{f_1 d_1}{f_1 - d_1}. \tag{4}$$

Substituting matrix elements from Eq. (3) into Eq. (2) with allowance for Eq. (4), we obtain the value of the complex parameter q_2, from where we can find the radius w of the beam and the radius R of the phase

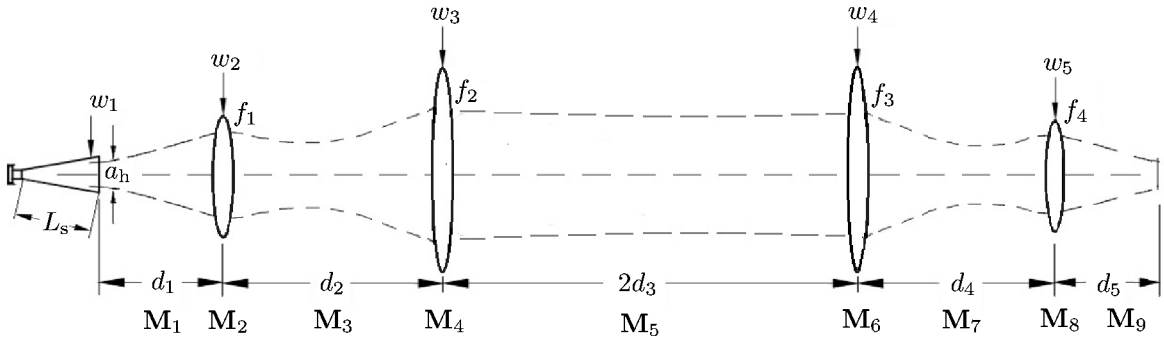

Fig. 3. Equivalent scheme of the Gaussian beam tracing. $\mathbf{M}_i$ are the ray matrices ($\mathbf{M}_2$, $\mathbf{M}_4 = \mathbf{M}_6$, and $\mathbf{M}_8$ are the ellipsoidal mirrors, presented here as lenses, with focal lengths f_1, f_2, and f_4), $w_1, \ldots, w_5$ are the beam radii on the elements of the optical system, $d_1, \ldots, d_5$ are the distances to mirrors, L_s is the horn length, and a_h is the horn aperture radius.

front curvature:

$$w_2 = \frac{f_1}{f_1 - d_1} w_1, \tag{5}$$

$$R_2 = \frac{R_1 {f_1}^2}{(f_1 - R_1 - d_1)(f_1 - d_1)}. \tag{6}$$

These equations show that the parameters of the Gaussian beam (phase curvature and beam radius) in the image planes of the optical system do not depend on frequency and coincide with the geometric-optical solution describing the single-lens transformation.

By solving the system of equations (4)–(6), we find the expressions and parameters used in what follows. Thus, free parameters w_3, R_3, w_1, and r_1 were selected for the "horn — second refocusing mirror" system. Then, the values of f_1, d_1, and d_2 were found using these parameters. Similarly, the "second refocusing mirror — Winston cone" system is calculated at the bolometer input.

The irradiating horn is one of the key elements of a quasi-optical system that determines its bandwidth and the quality of the formed beam, which is characterized by the coefficient of its matching with the fundamental Gaussian mode (gaussianity), the level of the side lobes, and the cross-polarization component. As is known, the optimal solution for the formation of a Gaussian beam is the use of a corrugated horn having a good gaussianity (about 98%), a low level of the cross-polarization component (-20 dB), and broadbandness (with a relative bandwidth of more than 50%) [16, 17, 22]. At the same time, it is the most laborious and high-tech device in terms of design and manufacture. Therefore, at this stage of the spectrometer upgrading, it was decided to use a diagonal horn [22–25] to assess the effect of providing a given irradiation level of a gas cell. A relatively high level of the cross-polarization component (about 10%) is suppressed by the grid polarizer in the quasi-optical path, provided for free use by the staff of the Submillimeter spectroscopy department directed by I. E. Spector from the Prokhorov General Physics Institute. Optimization of the gaussianity of the diagonal horn beam, which is about 84%, is achieved at $w = 0.43a_\mathrm{h}$, where a_h is the side length of a square at the horn opening [24]. In this case, the radius of the phase front curvature in the first approximation can be taken equal to the horn height ($R_1 = L_\mathrm{s}$).

Using specialized software for the finite element method, we performed three-dimensional electromagnetic modeling of the horn and additional optimization of its design. The layout of the horn in two planes is shown in Fig. 4. The diagonal horn and directional coupler were made from two mirror halves using split-block technology. When the horn, mirrors, and directional coupler were manufactured, a numerically controlled machine Roeders TEC RXP 500 DS was employed, which is part of the machinery equipment of the technological department at the IAP RAS. The manufacturing accuracy measured using a coordinate measuring machine WB-450DV Chien Wei was ± 3 μm. The flatness of the contact zone of the parts was 5 μm.

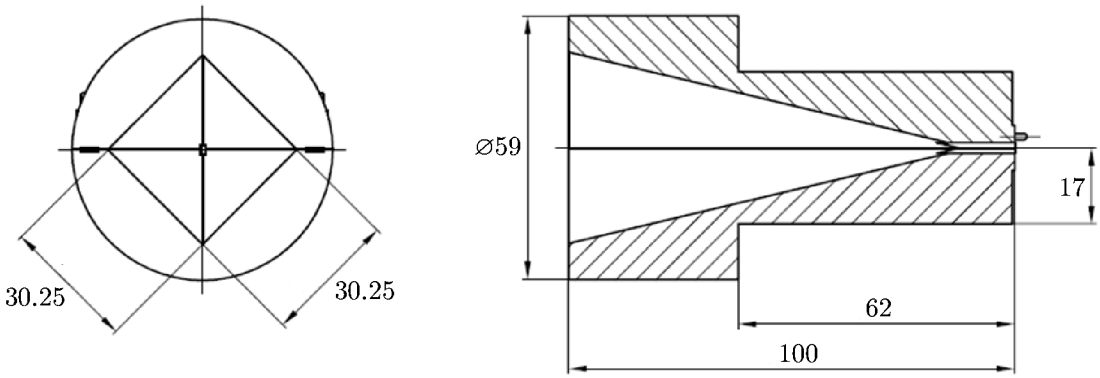

Fig. 4. Layout of the horn in two planes (the sizes are given in millimeters).

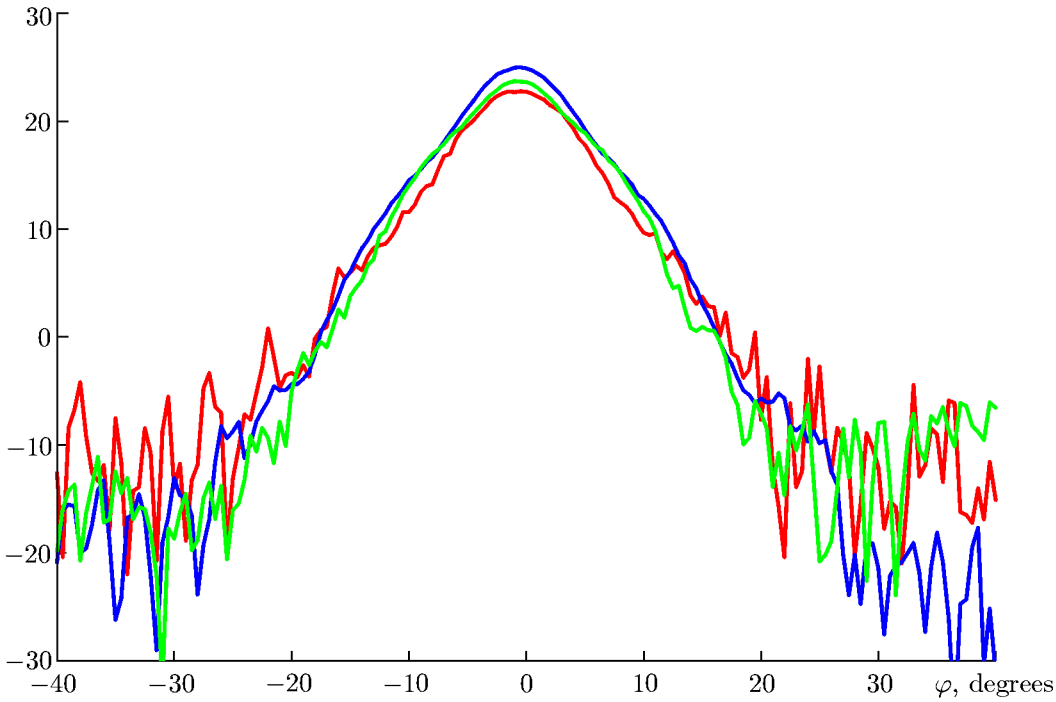

Fig. 5. Measured radiation pattern (in isotropic decibels) of the horn in the E plane at frequencies of 75 GHz (red curve), 90 GHz (blue curve), and 110 GHz (green curve).

We measured the characteristics of the horn in the far-field region in the anechoic chamber of the Sedakov Research Institute of Measuring Systems over the entire operating frequency range. As a result of measurements, it was found that the width of the main lobe of the radiation pattern and the gain differ by less than 2% in the range from 75 to 110 GHz (see Fig. 5).

Figure 6 shows comparative results of numerical calculations of the radiation pattern of the horn and measurements of its characteristics in the far-field region at a frequency of 90 GHz. The maximum of the radiation pattern was 25 dB, the level of the side lobes was −30 dB, and the width was 9° at the 3 dB level, in line with technical specification for the quasi-optical path of the spectrometer.

Since in our facility the cell is irradiated by a signal from a BWO, a phase-locked frequency system at an intermediate frequency of 395 MHz is used to synchronize the BWO with the reference oscillator (see Fig. 1). Within the framework of the creation of a new quasi-optical spectrometer, a directional coupler was designed for frequencies of 67–116 GHz. The split-block technology made it possible to construct waveguide channels for the coupler with a tolerance of 0.01 mm.

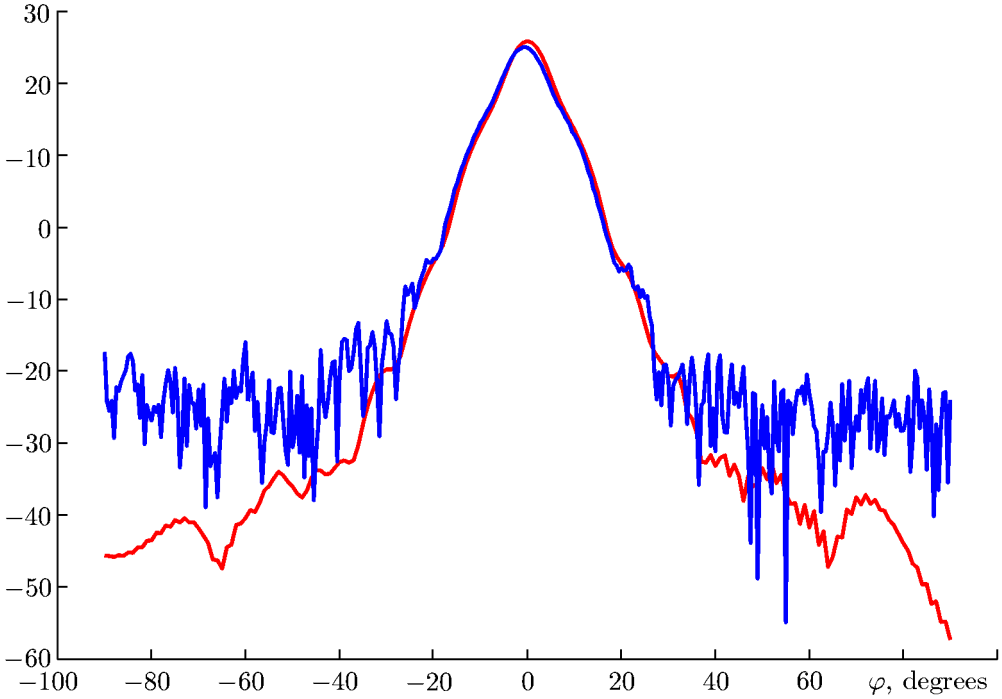

Fig. 6. Comparative results of numerical calculations of the radiation pattern (in isotropic decibels) of a horn in the E plane in CST Microwave Studio (red curve) and measurements of the horn characteristics in the far-field region in an anechoic chamber at a frequency of 90 GHz (blue curve).

3. LABORATORY STUDIES OF MOLECULAR SPECTRA

To study the capabilities of the created spectrometer, we performed measurements in the lines of purely rotational and torsion-rotational transitions of CH_3OH molecules, as well as hyperfine-split rotational transitions of CH_3CN and HNCO molecules. All measurements were carried out in the range 85–111 GHz. In this case, the spectra of CH_3CN were measured not only in the main, but also in the isotopologues of ^{13}C and ^{15}N in several vibrationally excited states. The main goals of these measurements, in addition to refining the transition frequencies and parameters of hyperfine splitting, also included the broadening and shifts of lines due to both pressure and radiation intensity. For this purpose, the measurements were performed in a fairly wide range of pressures (from tens to one-tenths of a millitorr) with radiation intensity varying by more than three orders of magnitude. As for the purely sub-Doppler regime, among other parameters characterizing the quality of such measurements, the spectral resolution is the main one. Thus, Fig. 3 in the paper by G. Cazzoli and C. Puzzarini [26] shows a record of a hyperfine-split transition in CH_3CN $J_K = 6_0$–5_0 at a frequency of 110 GHz to demonstrate the capabilities of their spectrometer.

Figure 7*a* shows the spectrum of this transition, which we measured in the regime where the cell was irradiated at the 18th harmonic of the frequency of the SMA100B oscillator, kindly provided to us by Rohde & Schwarz for test measurements. The tuning range of the oscillator is from 8 kHz to 20 GHz. The frequency used at the output of the amplification and multiplication chain producted by the Nizhny Novgorod branch of the Scientific and Production Association "Technoyaks" (Moscow) was scanned for the reduced transition near the frequency 6.132 GHz. To decrease the broadening of the lines by radiation, the oscillator power in front of the horn was attenuated by a factor of four using a calibrated attenuator. The signal was detected at the 2nd harmonic of the modulation frequency. In the case considered, internal modulation of the oscillator with a frequency of 1.5 kHz with a 9 kHz deviation at the line frequency was used. The gas pressure in the cell during measurements varied from 0.35 to 0.42 mTorr. In addition, measurements of the same line (see Fig. 7*b*) were carried out according to the scheme where the cell was irradiated using the OV-71 BWO

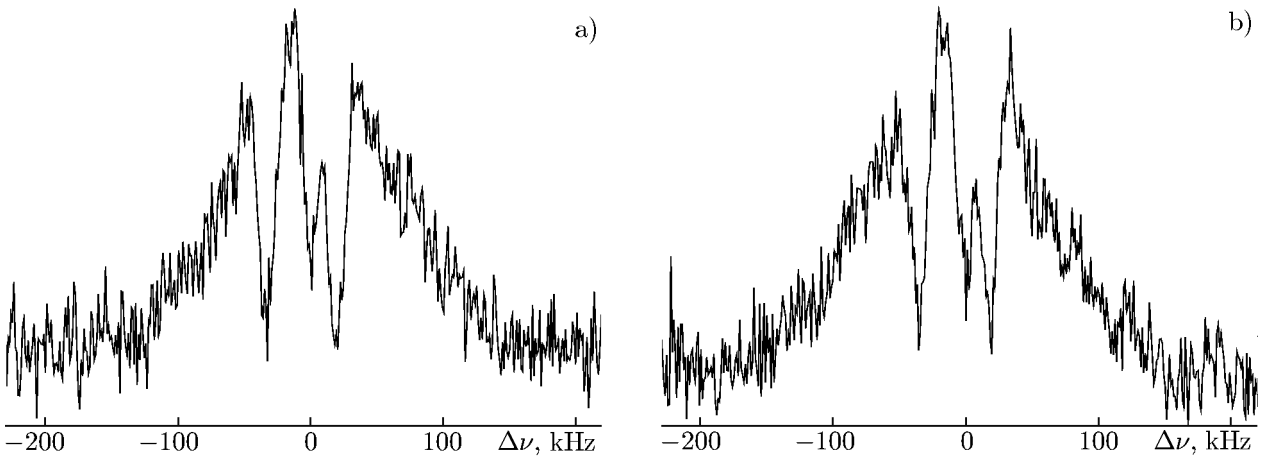

Fig. 7. (*a*) The hyperfine structure of the CH_3CN $J_K = 6_0 - 5_0$ transition at a frequency of 110 GHz, measured directly at the 18th harmonic of the Rohde & Schwarz SMA100B oscillator without using the BWO at an average gas pressure of 0.4 mTorr in the cell. (*b*) The same line measured when the cell was irradiated by the radiation from the OV-71 BWO stabilized at the 18th harmonic of the KeySight Technologies E8257D oscillator at a pressure of 0.5 mTorr. Both records are reduced to the same scale. The attenuation of radiation is 6 dB and 21 dB (*a* and *b*, respectively).

produced by the A. I. Shokin JSC Scientific and Production Enterprise "Istok." The BWO was stabilized by the 18th harmonic of the E8257D synthesizer, kindly provided to us by Keysight Technologies for test measurements. In this case, frequency modulation with the same parameters was fed to a synchronizer manufactured at the IAP RAS with an intermediate frequency of 395 MHz and formed by the Rohde & Schwarz HMF2550 oscillator. Since the rated capacity of the BWO was close to 30 MW, its power was attenuated by more than two orders of magnitude. Both schemes showed almost identical results.

The above figures show that our resolution capabilities are not inferior to the G. Cazzali and C. Puzzarini's spectrometer, although the cell length is twice as short. As for the sensitivity to weak lines, it must be said that we measured this transition with a Lamb dip in the natural content of isotopologues not only in $CH_3^{13}CN$, but also in $CH_3C^{15}N$. The corresponding abundance of the $^{13}C/^{12}C$ and $^{15}N/^{14}N$ isotopes is approximately 1/90 and 1/270 [27].

Figure 8 shows the hyperfine structure of the rotational transition $J_{K_a,K_c} = 4_{0.4} - 3_{0.3}$ in the HNCO molecule at a frequency of 88 GHz for a gas pressure in the cell about 0.6 mTorr. As the initial frequency of the rotational transition, we used our own value measured by a spectrometer based on the radio-acoustic detection principle [28]. As in the case of CH_3CN $J_K = 6_0 - 5_0$, only the central group of components is given against the background of a wide Doppler contour stipulated by thermal velocities of the molecules. The modulation frequency is also equal to 1.5 kHz and the deviation is 5 kHz. Since in this case the cell was irradiated using the OV-71 BWO, stabilized by the 18th harmonic of the SMA100A oscillator, we had to introduce additional attenuation by a calibrated attenuator to reduce the line broadening by radiation. It is clearly seen that the maximum frequency resolution is observed when the BWO is attenuated by about two orders of magnitude, while the ratio between the noise level and the signal amplitude in the line remains almost unchanged over a wide attenuation range. Despite the extremely low deviation frequency, the characteristic time of measurement of one record with allowance for the pressure adjustment, was quite small and amounted to about 15 min. It is also seen that the signal-to-noise ratio in the records decreases not only at a very low, but also a high radiation power, which is caused by the features of frequency modulation with increasing line width due to saturation by radiation.

The results of the performed measurements will be presented in more detail in the further publications.

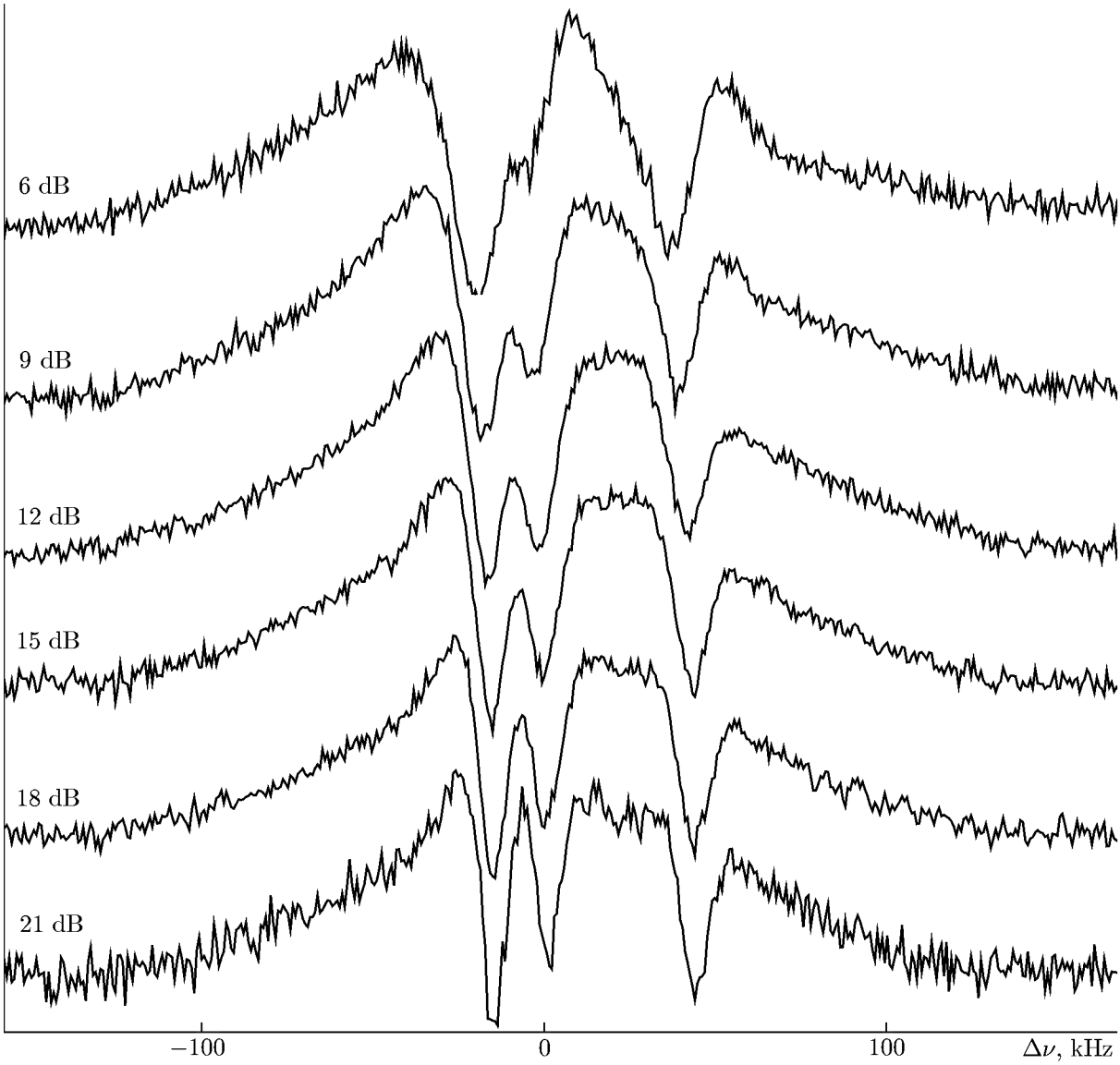

Fig. 8. Example of sub-Doppler Lamb-gap measurements of hyperfine splitting of the HNCO rotational transition $J_{K_a,K_c} = 4_{0.4} - 3_{0.3}$ at a frequency of 87925 MHz for a pressure of about 0.6 mTorr. The measurements are recorded at the second harmonic of the modulation frequency at 1.5 kHz with a 5 kHz deviation. An increase in spectral resolution is clearly seen as the BWO power is decreased from 6 to 21 dB due to a decrease in the line broadening by radiation. All records are reduced to the same scale.

4. CONCLUSIONS

A new sub-Doppler spectrometer of millimeter and submillimeter wavelength ranges with a gas cell having a diameter of 40 cm has been developed for high-precision laboratory measurements of molecular transitions by the Lamb-dip method. The principle of frequency-independent irradiation of the cell was implemented in the manufacture of the optical scheme of the spectrometer. As a result of the performed studies, it was found that the spectral resolution of the spectrometer corresponds to the best laboratory measurements in the millimeter frequency range required for radio astronomy, molecular spectroscopy, and fundamental astrophysical research. By reducing the optical length of a cell while increasing simultaneously its diameter for the lines of molecules with large dipole momenta, distortions in the shape of absorption profiles have been eliminated due to the optical depth. By decreasing the modulation frequency when using

oscillators with lower phase noise and shorter cell length, the absorption profile distortions stipulated by phase delays during radiation propagation have been removed.

The authors of this paper express their gratitude to A. A. Dityatev, Yu. F. Avdeev, and A. I. Torgovanov from Rohde & Schwarz Rus, as well as A. S. Danilov from Keysight Technologies for providing frequency oscillators during tests and consultations during measurements. The work was supported by the Ministry of Science and Higher Education of the Russian Federation (State assignment under topic No. 0030–2021 –0005) and the Russian Science Foundation (project No. 17–12–01256).

REFERENCES

1. G. Cazzoli, C. Puzzarini, and A. V. Lapinov, *Astrophys. J.*, **592**, L95–L98 (2003). https://doi.org/10.1086/377527
2. G. Cazzoli, C. Puzzarini, and A. V. Lapinov, *Astrophys. J.*, **611**, 615–620 (2004). https://doi.org/10.1086/421992
3. A. V. Lapinov, *Proc. SPIE*, **6580**, 658001 (2006). https://doi.org/10.1117/12.724761
4. F. J. Lovas, *J. Phys. Chem. Ref. Data*, **33**, 177–355 (2004). https://doi.org/10.1063/1.1633275
5. V. S. Letokhov and V. P. Chebotaev, *Ultra-High Resolution Nonlinear Laser Spectroscopy* [in Russian], Nauka, Moscow (1990).
6. G. Yu. Golubyatnikov, S. P. Belov, I. I. Leonov, et al., *Radiophys. Quantum Electron.*, **56**, Nos. 8–9, 599–609 (2014). https://doi.org/10.1007/s11141-014-9464-2
7. G. Yu. Golubyatnikov, S. P. Belov, and I. I. Leonov, *Radiophys. Quantum Electron.*, **58**, No. 8, 622–631 (2015). https://doi.org/10.1007/s11141-016-9634-5
8. S. P. Belov, G. Yu. Golubiatnikov, A. V. Lapinov, et al., *J. Chem. Phys.*, **145**, No. 2, 024307 (2016). https://doi.org/10.1063/1.4954941
9. L.-H. Xu, J. T. Hougen, G. Yu. Golubiatnikov, et al., *J. Mol. Spectrosc.*, **357**, 11–23 (2019). https://doi.org/10.1016/j.jms.2018.12.003
10. G. Cazzoli and L. Dore, *J. Mol. Spectrosc.*, **141**, 49–58 (1990). https://doi.org/10.1016/0022-2852(90)90277-W
11. G. Winnewisser, S. P. Belov, Th. Klaus, and R. Schieder, *J. Mol. Spectrosc.*, **184**, 468–472 (1997). https://doi.org/10.1006/jmsp.1997.7341
12. G. Yu. Golubiatnikov, A. V. Lapinov, A. Guarnieri, and R. Knöchel, *J. Mol. Spectrosc.*, **234**, 190–194 (2005). https://doi.org/10.1016/j.jms.2005.08.012
13. E. A. Alekseev, V. V. Ilyushin, and A. A. Meshcheryakov, *Radiophys. Radioastr.*, **19**, No. 4, 364–374 (2014). https://doi.org/10.15407/rpra19.04.364
14. L.-H. Xu, E. M. Reid, B. Guislain, et al., *J. Mol. Spectrosc.*, **342**, 116–124 (2017). https://doi.org/10.1016/j.jms.2017.06.008
15. J. Lamb, *Optical Study for ALMA Receivers. ALMA Memo 359*, North American ALMA Science Center, Charlottesville (2001).
16. I. Lapkin, O. Nyström, V. Desmaris, et al., in: *Proc. 19th Int. Symp. Space Terahertz Technology, April 28–30, 2008, Groningen, Netherlands*, P. 351–357.
17. O. Nyström, I. Lapkin, V. Desmaris, et al., *J. Infrared Millim. Terahertz Waves*, **30**, 746–761 (2009). https://doi.org/10.1007/s10762-009-9493-7
18. Goldsmith P. F., in: K. J. Button, ed., *Infrared and Millimeter Waves*, Vol. 6, Academic Press, New York (1982), p. 277–344.

19. P. F. Goldsmith, *Quasioptical Systems: Gaussian Beam Quasioptical Propagation and Applications*, IEEE Press, New York (1998).

20. O. Svelto, *Principles of Lasers*, Plenum, New York (1989).

21. T.-S. Chu, *IEEE Trans. Antennas Propag.*, **AP-31**, No. 4, 614–619 (1983). https://doi.org/10.1109/TAP.1983.1143090

22. G.-Q. Wang and S.-C. Shi, in: *Proc. Global Symp. Millimeter Waves, April 21–24, 2008, Nanjing, China*, 4534598. https://doi.org/10.1109/GSMM.2008.4534598

23. A. W. Love, *Microwave J.*, **5**, 117–122 (1962).

24. J. F. Johansson, N. Whyborn, P. R. Acharya, et al., in: *Proc. 2nd Int. Symp. Space Terahertz Tech., February 26–28, 1991, Pasadena, USA*, pp. 63–69.

25. S. Withington and J. A. Murphy, *IEEE Trans. Antennas Propag.*, **40**, 198–206 (1992). https://doi.org/10.1109/8.127404

26. G. Cazzoli and C. Puzzarini, *J. Mol. Spectrosc.*, **240**, 153–163 (2006). https://doi.org/10.1016/j.jms.2006.09.013

27. J. Emsley, *The Elements*, Clarendon Press, London (1991).

28. A. V. Lapinov, G. Yu. Golubiatnikov, V. N. Markov, and A. Guarnieri, *Astron. Lett.*, **33**, No. 2, 121–129 (2007). https://doi.org/10.1134/S1063773707020065